ChemMedChem

Chemistry Europe
European Chemical Societies Publishing

Accepted Article

Title: Matrix Metalloproteinase 13 Inhibitors for Modulation of Osteoclastogenesis: Enhancement of Solubility and Stability

Authors: Gregg Fields, Anna M. Knapinska, Chandani Singh, Gary Drotleff, Daniela Blanco, Cedric Chai, Jason Schwab, and Anu Herd

To be cited as: *ChemMedChem* 10.1002/cmdc.202000911

Link to VoR: https://doi.org/10.1002/cmdc.202000911

WILEY-VCH

WILEY-VCH

FULL PAPER

Matrix Metalloproteinase 13 Inhibitors for Modulation of Osteoclastogenesis: Enhancement of Solubility and Stability

Anna M. Knapinska,[a,c] Chandani Singh,[a,c] Gary Drotleff,[b] Daniela Blanco,[c] Cedric Chai,[b] Jason Schwab,[c] Anu Herd,[c] and Gregg B. Fields*[a,c,d]

[a] Dr. A.M. Knapinska, C. Singh, Prof. G.B. Fields
Department of Chemistry & Biochemistry
Florida Atlantic University
5353 Parkside Drive, Jupiter, FL 33458
E-mail: fieldsg@fau.edu

[b] G. Drotleff, C. Chai
Department of Biological Sciences
Florida Atlantic University
777 Glades Road, Boca Raton, FL 33431

[c] Dr. A.M. Knapinska, C. Singh, D. Blanco, J. Schwab, A. Herd, Prof. G.B. Fields
Institute for Human Health & Disease Intervention (I-HEALTH)
Florida Atlantic University
5353 Parkside Drive, Jupiter, FL 33458

[d] Prof. G.B. Fields
Department of Chemistry
The Scripps Research Institute/Scripps Florida
120 Scripps Way, Jupiter, FL 33458

Supporting information for this article is given via a link at the end of the document.

Abstract: Matrix metalloproteinase 13 (MMP-13) activity has been correlated to breast cancer bone metastasis. It has been proposed that MMP-13 contributes to bone metastasis via promotion of osteoclastogeneis. To explore the mechanisms of MMP-13 action, we previously described a highly efficacious and selective MMP-13 inhibitor, RF036. Unfortunately, further pursuit of RF036 as a probe of MMP-13 *in vitro* and *in vivo* activities was not practical due to the limited solubility and stability of the inhibitor. The present study has explored replacement of the RF036 backbone sulfur atom and terminal methyl group to create inhibitors with more favorable pharmacokinetic properties. One compound, designated inhibitor 3, in which the backbone sulfur and terminal methyl group of RF036 were replaced by nitrogen and oxetane, respectively, had comparable activity, selectivity, and membrane permeability to RF036 while exhibiting greatly enhanced solubility and stability. Inhibitor 3 effectively inhibited MMP-13-mediated osteoclastogenesis but spared collagenolysis, and thus represents a next generation MMP-13 probe applicable for *in vivo* studies of breast cancer metastasis.

Introduction

Analysis of The Cancer Genome Atlas (TCGA) data found that the protease matrix metalloproteinase 13 (MMP-13) was almost universally upregulated across 15 different cancer types, with significant upregulation in 12 cancers, including breast cancer (BRCA).[1] MMP-13 was originally isolated and cloned from breast carcinomas.[2] Microarray analysis of genes from infiltrating lobular carcinoma, metaplastic carcinoma, and infiltrating ductal carcinoma of breast cancer patients revealed 100% overexpression of MMP-13.[3] MMP-13 was secreted as a protein in pro and active forms.[3] MMP-13 protein levels correlated with lymph node metastasis of breast cancer and inversely with patient survival.[4]

Upon autopsy 70-80% of women that succumb to breast cancer have evidence of bone metastases.[5] The metastases generate extensive bone destruction as a result of uncontrolled osteoclast activity, causing the patient great pain and contributing significantly to the morbidity associated with the disease. Breast cancer cells may induce the expression of potent osteoclastogenic factors, such as receptor activator of nuclear kappa B (NF-κB) ligand (RANKL), by bone-lining osteoblasts.[6] Inoculation of nude mice with MDA-MB-231 breast cancer cells resulted in osteoclasts resorbing bone, degradation of bone matrix, and metastasis.[7] The expression of RANKL, MMP-13, and MT1-MMP mRNA was increased in the metastasized bone, and MMP-13 protein was found in breast cancer bone metastases.[7-8] Subsequently, MMP-13 in MDA-MB-231 breast cancer cells was found to be responsible for increased bone resorption and osteoclastogenesis, which was reduced by the application of MMP inhibitors.[8] The MMP-13 inhibitor 5-(4-{4-[4-(4-fluorophenyl)-1,3-oxazol-2-yl]phenoxy}phenoxy)-5-(2-methoxyethyl)-pyrimidine-2,4,6 (1H,3H,5H)-trione (compound 28 in [9]) inhibited MDA-MB-231 breast cancer xenograft growth and significantly reduced osteolytic damage in an *in vivo* prevention study.[10] The inhibitor did not cause an increase in creatine kinase, a measure of muscle toxicity.[10]

Concern has been raised that many anti-cancer drugs undergoing clinical trials actually function by off-target toxicity.[11] Prior MMP inhibitors, particularly those possessing hydroxamic groups which target the active site zinc, have been shown to have considerable off-target activities.[12] To counteract this behavior, selective, non-zinc chelating MMP-13 inhibitors have been described.[9-10, 13] However, important pharmacokinetic (PK) and/or other data has not been reported for many of these compounds, and no clinical studies have appeared. Some of the most promising recent selective MMP-13 inhibitors had nephrotoxicity and/or poor solubility, permeability, biodistribution,

metabolic stability, and/or bioavailability and thus the search for new MMP-13 inhibitors continues.[13o, 13p]

Our laboratory has developed a series of small molecules that are highly selective for MMP-13 with IC_{50} values in the low nM range (2.7-5.9 nM).[14] RF036 (compound **(*S*)-17b** in [14a] and compound **2** in [14b]) (Figure 1) has an IC_{50} of 3.4-4.9 nM for MMP-13 and is highly selective. RF036 displayed an excellent permeability profile in Caco-2 based membrane permeability studies, with P_{app}= 2.38 x 10^{-6} cm/sec. RF036 had a long plasma half-life time ($T_{1/2}$ = 2.93 h), high maximum plasma concentration (C_{max} = 47.6 μM), and low clearance rate (Cl = 0.18 mL/min/kg) after intravenous administration in rats. However, compound RF036 suffers from poor metabolic stability when incubated with mouse, rat, and human liver microsomes, and its solubility is marginal for *in vivo* applications. The present research selectively targets RF036 areas of potential instability and replaces them with more stable bonds and moieties, while also seeking to improve compound solubility. The overall goal is to create a highly stable, first in class agent that targets MMP-13 in breast cancer.

Results and Discussion

Synthesis of MMP-13 Inhibitors

Inhibitor oral bioavailability can be improved by increasing compound (a) solubility, (b) cell permeability, and (c) metabolic stability.[15] RF036 has a fairly low kinetic solubility of 15.5 μM.[14b] RF036 is moderately cell permeable (2.38 x 10^{-6} cm/sec) with retention fraction in the lipid bilayer of 47%,[14b] which indicates that oral bioavailability could be restricted through limited diffusion of the compound through and retention of the compound in the gastrointestinal wall. The *in vitro* $t_{1/2}$ of RF036 was only 9 min in human microsomes,[14b] which means that low oral bioavailability could result from degradation of the compound by CYP450 dependent metabolizing enzymes. There are two obvious areas of potential instability in compound RF036, the sulfur and the methylamine (Figure 1).[14b] Replacement of the sulfur by either a carbon or a nitrogen only slightly altered the MMP-13 inhibitory activity of the resulting compounds but improved stability in human microsomes.[14b] Replacement of the methyl group in the methylamine by heteroatom cyclic butane analogs also only slightly altered the MMP-13 inhibitory activity of the resulting compounds but improved stability in human microsomes.[14b]

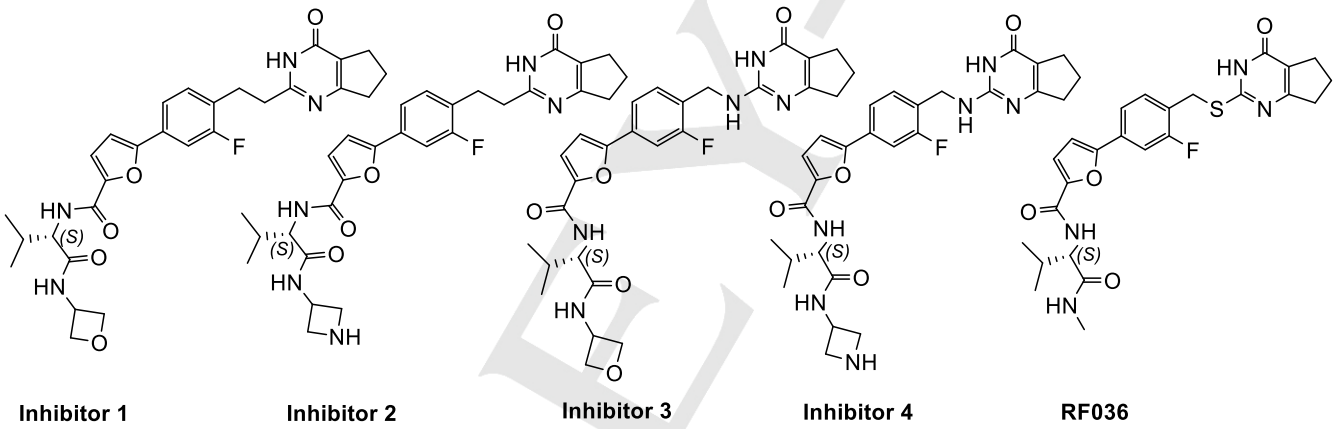

Figure 1. Structures of Inhibitors 1-4 and RF036.

In the present study, the sulfur from RF036 was replaced with carbon (inhibitor 1 and inhibitor 2) or nitrogen (inhibitor 3 and inhibitor 4) and the methyl in the methylamine group was replaced with oxetane (1,3-propylene oxide) (inhibitor 1 and inhibitor 3) or azetidine (1,3-propylenimine) (inhibitor 2 and inhibitor 4) (Figure 1). For the synthesis of inhibitor 1 and inhibitor 2 (Scheme 1), steps from compound **1** to compound **8** were identical to those from compound **57** to compound **61** as described previously.[14b] Synthesis of compound **9** from compound **8** was the same as treatment of compound **61**, step 1), in Scheme 6 of our prior study.[14b] For the synthesis of compound **10** from compound **9**, L-valine methyl ester hydrochloride was reacted with compound **9** using EDCI•HCl, HOBt, and NEt_3. Synthesis of compound **11** from compound **10** was the same as treatment of compound **7**, step 1), in Scheme 1 of our prior study.[14b] For the synthesis of inhibitor 1 from compound **11**, oxetan-3-amine was reacted with compound **11** using EDCI•HCl, HOBt, and DIPEA. For the synthesis of inhibitor 2 from compound **11**, *tert*-butyl 3-aminoazetidine-1-carboxylate was reacted with compound **11** using EDCI•HCl, HOBt, and DIPEA, followed by removal of the Boc group with TFA treatment for 3 h at room temperature.

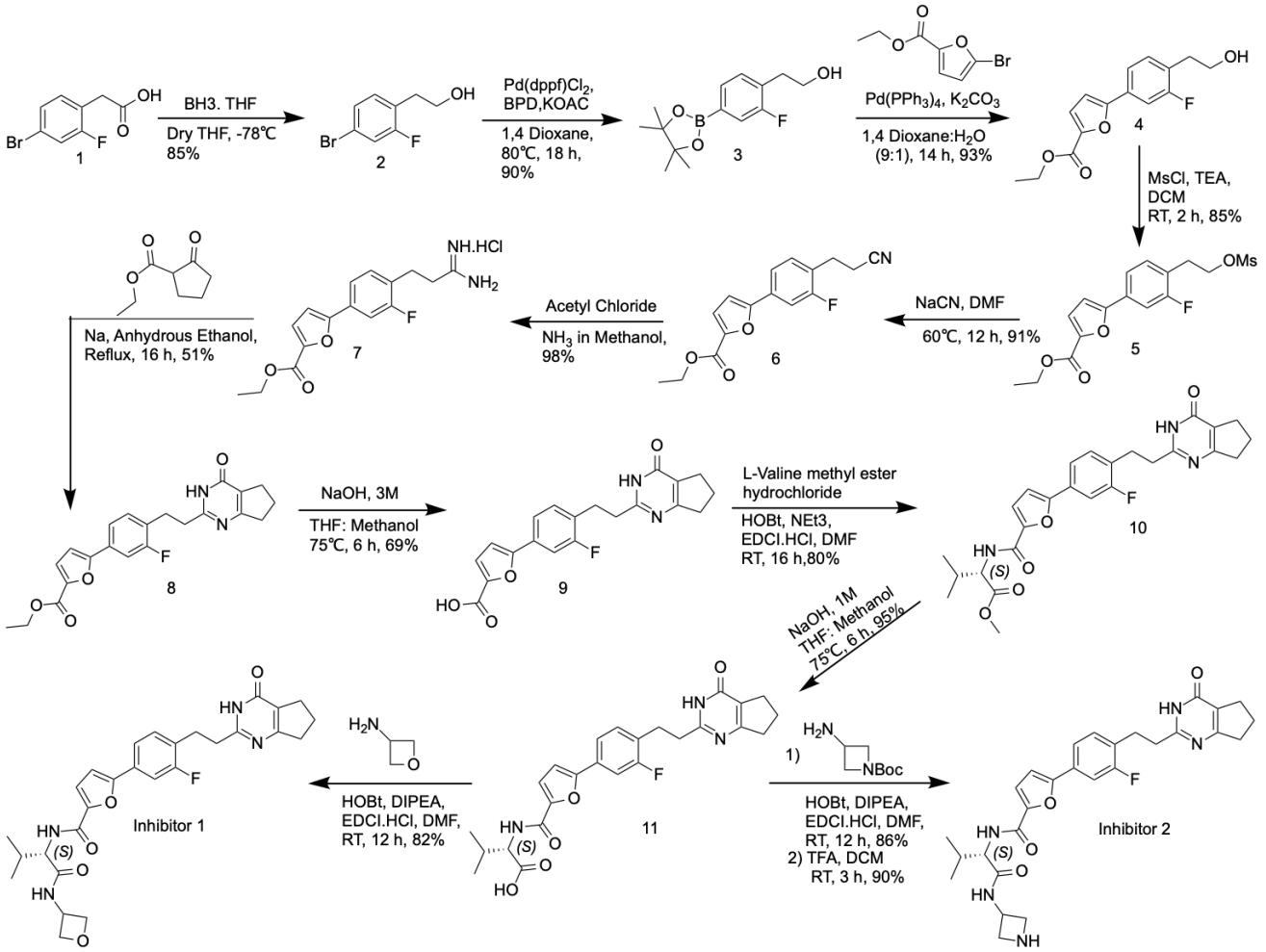

Scheme 1. Synthesis of Inhibitors 1 and 2.

Compound **17** (2-chloro-1,5,6,7-tetrahydro-4*H*-cyclopenta[*d*]pyrimidin-4-one) was synthesized starting from ethyl-2-oxo-cyclopentane-carboxylate (Scheme 2). Ethyl-2-oxo-cyclopentane-carboxylate was reacted with urea and concentrated HCl for 4 h at 80 °C, and the product was heated with NaOH for 1.5 h at 110 °C. After acidifying with 2 M HCl, compound **17a** was obtained. Compound **17a** was reacted with phosphorus oxychloride for 2 h at 120 °C to provide compound **17b**.

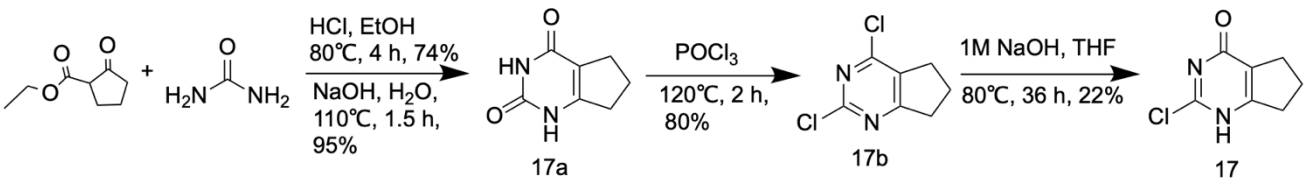

Scheme 2. Synthesis of intermediate 17.

For the synthesis of inhibitor 3 and inhibitor 4 (Scheme 3), steps from compound **12** to compound **18** were identical to those from compound **62** to compound **67** as described previously.[14b] Synthesis of compound **19** from compound **18** was the same as treatment of compound **67**, step 1), in Scheme 6 of our prior study.[14b] For the synthesis of compound **20** from compound **19**, L-valine methyl ester hydrochloride was reacted with compound **19** using EDCI•HCl, HOBt, and NEt_3. For the synthesis of compound **21** from compound **20**, compound **20** was treated with 2 M NaOH for 8 h at 75 °C. For the synthesis of inhibitor 3 from

compound **21**, oxetan-3-amine was reacted with compound **21** using EDCI•HCl, HOBt, and DIPEA. For the synthesis of compound **22** from compound **21**, *tert*-butyl 3-aminoazetidine-1-carboxylate was reacted with compound **21** using EDCI•HCl, HOBt, and DIPEA. For the synthesis of inhibitor 4 from compound **22**, compound **22** was treated with TFA for 4 h at room temperature.

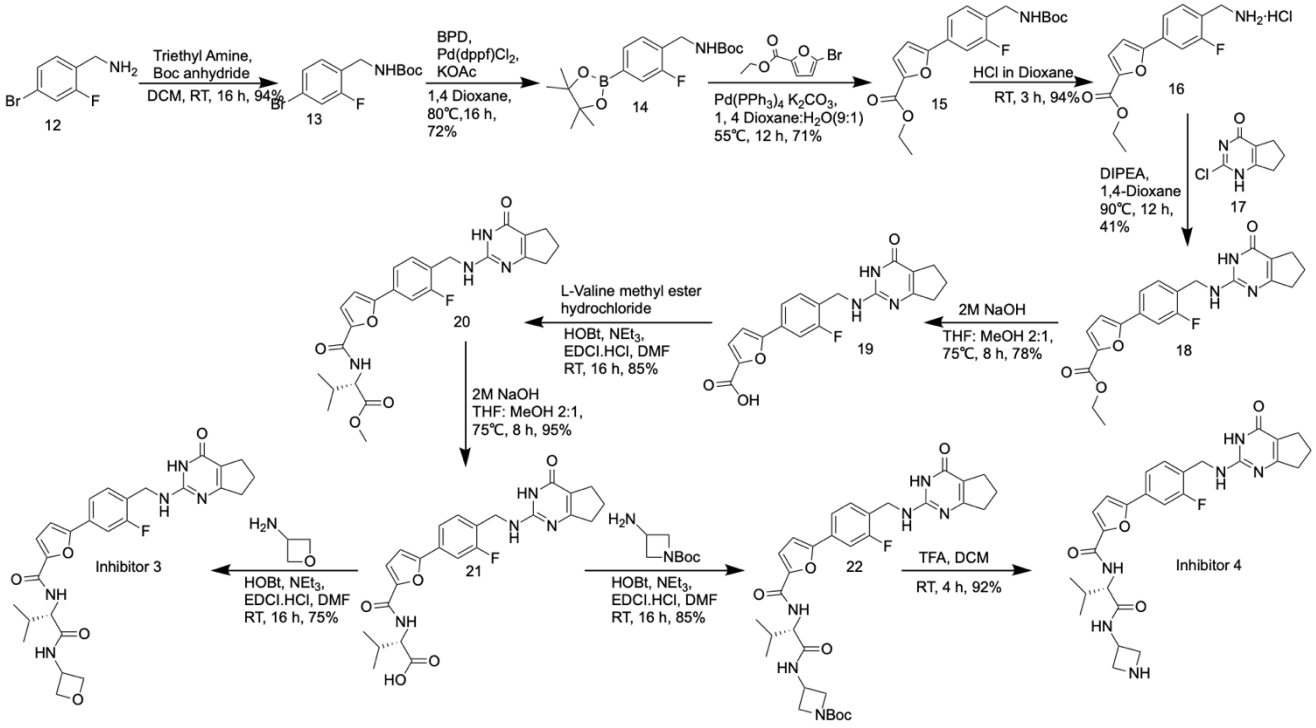

Scheme 3. Synthesis of Inhibitors 3 and 4.

MMP Activity of Inhibitors

Compounds were initially screened for their activity against MMP-13 and their selectivity for MMP-13 versus MMP-1, MMP-2, MMP-8, MMP-9, and MMP-14/MT1-MMP (Table 1). Inhibitor 1, inhibitor 2, and inhibitor 3 were all effective inhibitors of MMP-13, with K_i values of 12, 42, and 10 nM, respectively (Table 1). The values for inhibitor 1 and inhibitor 3 are comparable to the parent compound, RF-036 (K_i = 2.7 nM).[14] Inhibitors 1, 2, and 3 all had selectivity comparable to that observed with RF-036, as the IC_{50} values for other MMPs were greater than 5 μM (Table 1). RF036 had IC_{50} values of >5 μM for MMP-1, MMP-2, MMP-8, MMP-9, and MMP-14/MT1-MMP.[14]

Table 1. Inhibition of MMPs.

Compound	MMP-13 K_i (nM)	MMP-1 IC_{50} (nM)	MMP-2 IC_{50} (nM)	MMP-8 IC_{50} (nM)	MMP-9 IC_{50} (nM)	MMP-14 IC_{50} (nM)
RF036[a]	2.7 ± 0.6	>5000	>5000	>5000	>5000	>5000
Inhibitor 1	12.2 ± 0.8	>5000	>5000	>5000	>5000	>5000
Inhibitor 2	41.9 ± 3.6	>5000	>5000	>5000	>5000	>5000
Inhibitor 3	10.3 ± 0.6	>5000	>5000	>5000	>5000	>5000
Inhibitor 4	28.1 ± 1.5[b] 63.7 ± 1.5[c] 74[d] 134[d] 334[d] 347[d] 544[d] 677[d] 1600[d]	>5000	>5000	>5000	>5000	>5000

[a]RF036 values were previously reported.[14a]
[b]TFA salt; [c]TFA salt after 3 month storage in DMSO; [d]formic acid salt form over 3 month time period storage in DMSO.

Inhibitor 4 had variable activity against MMP-13. For example, when inhibitor 4 was produced as the formic acid salt, the IC_{50} values for MMP-13 increased over time, from 74 nM to 1.6 μM (Table 1). When stored as a stock solution in DMSO at -20 °C, LC-MS analysis indicated significant decomposition of the formic acid form of inhibitor 4 after 5-7 days. When inhibitor 4 was produced as the TFA salt, the stability in DMSO was improved (as monitored by LC-MS), but nonetheless the IC_{50} value increased from 28 to 64 nM over time (Table 1). Inhibitor 4 was found to

have better stability when stored as a stock solution in EAB and frozen.

Overall, inhibitor 1 and inhibitor 3 retained better inhibitory activity towards MMP-13 than inhibitor 2 and inhibitor 4. Thus, the azetidine resulted in somewhat inferior inhibition compared with the oxetane. This result is consistent with the prior study where the parent compound (RF036) methyl group was replaced by either oxetane (IC_{50} went from 2.7 to 4.4 nM) or azetidine (IC_{50} went from 2.7 to 20 nM).[14b]

Drug Metabolism and Pharmacokinetic Profile of MMP-13 Inhibitors

The kinetic solubilities of each compound were evaluated. Inhibitors 1 and 3 exhibited kinetic solubilities of 39.9 ± 7 (76.4 ± 13.4 μM) and 17.1 ± 1 (32.7 ± 1.9 μM) μg/mL, respectively, which are considered moderate solubilities (Table 2). Inhibitors 2 and 4 exhibited kinetic solubilities of 275 ± 0.1 (484.5 ± 0.2 μM) and 216 ± 5 (379.9 ± 8.8 μM) μg/mL, respectively, which are considered high solubilities (Table 2). The azetidine in inhibitors 2 and 4 clearly enhanced solubility compared with the oxetane in inhibitors 1 and 3. RF036 (MW = 499.17 g/mol) had a solubility of 15.5 μM = 7.74 μg/mL,[14b] which is considered poor solubility (<10 μg/mL or <20 μM). All four compounds had greatly improved solubility compared with RF036 (Table 2).

Table 2. Pharmacokinetic Properties of MMP-13 Inhibitors.

Compound	Kinetic solubility (μM)	Human microsome half-life (min)	Rat microsome half-life (min)	Mouse microsome half-life (min)	Caco-2 cell permeability P_{app} (x 10^{-6} cm/sec)
RF036[a]	15.5	12	9	20	2.38
Inhibitor 1	76.4 ± 13.4	61.4 ± 8.3	61.9 ± 4.4	103.6 ± 7.5	2.3 ± 1.9
Inhibitor 2	484.5 ± 0.2	266.7 ± 89.9	593.2 ± 33.7	119.7 ± 35.4	0.98 ± 0.28
Inhibitor 3	32.7 ± 1.9	66.0 ± 14.8	99.9 ± 18.2	94.8 ± 0.8	1.9 ± 0.3
Inhibitor 4	379.9 ± 8.8	158.4 ± 29.8	160.1 ± 20.6	353.6 ± 221.0	2.3 ± 1.1

[a]RF036 values were previously reported.[14b]

The stability of inhibitors 1, 2, 3, and 4 were compared in human, rat, and mouse microsomes (Table 2). The $t_{1/2}$ for inhibitor 1 in human, rat, and mouse microsomes was 61.4 ± 8.3, 61.9 ± 4.4, and 103.6 ± 7.5 min, respectively. The $t_{1/2}$ for inhibitor 2 in human, rat, and mouse microsomes was 266.7 ± 89.9, 593.2 ± 33.7, and 119.7 ± 35.4 min, respectively. The $t_{1/2}$ for inhibitor 3 in human, rat, and mouse microsomes was 66.0 ± 14.8, 99.9 ± 18.2, and 94.8 ± 0.8 min, respectively. The $t_{1/2}$ for inhibitor 4 in human, rat, and mouse microsomes was 158.4 ± 29.8, 160.1 ± 20.6, and 353.6 ± 221.0 min, respectively. The $t_{1/2}$ for verapamil in human, rat, and mouse microsomes was 6.62 ± 0.28, 5.42 ± 0.02, and 7.60 ± 0.07 min, respectively. All inhibitors had greatly improved stability compared with RF036, which had a $t_{1/2}$ of 12, 9, and 20 min in human, rat, and mouse microsomes, respectively.[14b] Compounds with oxetane were, in general, less stable then compounds with azetidine. This result is consistent with the prior study where the parent compound (RF036) Me group was replaced by either oxetane or azetidine.[14b]

Membrane permeability was studied using Caco-2 cells. Active permeability mechanisms can be evaluated with the Caco-2 assay[16] because human epithelial colorectal adenocarcinoma cells, which imitate the epithelial cell layer of the small intestine, express membrane proteins such as P-glycoprotein (Pgp), breast cancer resistance protein (BCRP), and multidrug resistance protein 2 (MRP2) on the apical surface. Efflux transporters expressed in the apical membrane of intestinal enterocytes have been implicated in drug oral absorption. For compounds where active efflux impacts permeability, the inherent passive membrane permeability ("intrinsic permeability") gives a measure of the compound's permeability.[17] Apical to basal P_{app} was 2.3 ± 1.9, 0.98 ± 0.28, 1.9 ± 0.3, and 2.3 ± 1.1 x 10^{-6} cm/sec for inhibitors 1, 2, 3, and 4, respectively (Table 2). Inhibitors 1, 3, and 4 were considered to have medium permeability, which is defined as between 1.5 and 10 x 10^{-6} cm/sec, while inhibitor 2 was considered to have low permeability. RF036 had a permeability of 2.38 x 10^{-6} cm/sec.[14b] Thus, inhibitors 1, 3, and 4 had comparable membrane permeability to RF036.

Inhibition of Osteoclastogenesis and Collagenolysis

MMP-13 has been described previously as contributing to mesenchymal stem cell (MSC) osteogenic differentiation.[18] RF036 was found to inhibit osteoclast formation in a dose-dependent fashion in bone marrow co-cultures that contained bone MSCs (manuscript submitted). The action of RF036 was not due to the compound being toxic towards monocytes, MSCs, or mature osteoclasts, even at a concentration of 10 μM (manuscript submitted). The present inhibitors 1-4 were tested at a concentration of 10 μM and compared with RF036 for inhibition of osteoclastogenesis (Figure 2). Inhibitors 1 and 3 inhibited osteoclastogenesis to levels of 28 and 22%, respectively, similar to 24% observed for RF036 (Figure 2). Inhibitor 4 treatment resulted in 31% osteoclastogenesis, while inhibitor 2 was relatively ineffective at inhibiting osteoclastogenesis (79% activity compared with control) (Figure 2). The lack of cell debris indicated that none of the inhibitors were cytotoxic.

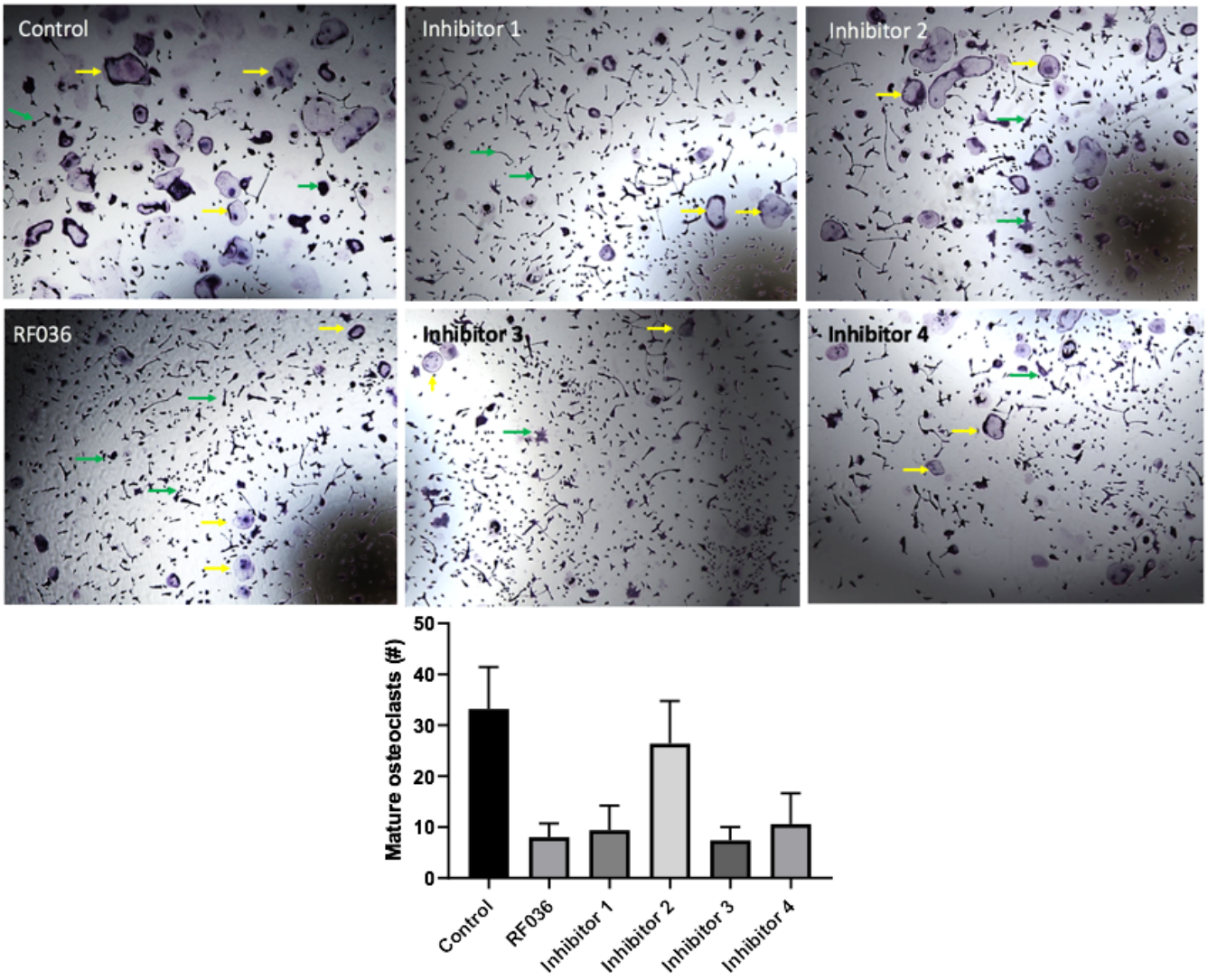

Figure 2. Inhibition of osteoclastogenesis by RF036 and inhibitors 1-4. Bone mesenchymal stem cells were plated at 1 x 10^5 cells/250 μL/well in a 48 well plate in fresh media containing 25 ng/mL rM-CSF and 100 ng/mL RANKL. Inhibitors were added in triplicates at 10 μM final concentration at the time of plating. Media was refreshed every 2-3 d for 5-7 d. Representative mature osteoclasts are indicated with yellow arrows while representative undifferentiated MSCs and immature osteoclasts are indicated with green arrows.

While the present and prior studies have shown that MMP-13 facilitates osteoclastogenesis, the mechanism by which MMP-13 acts is unknown. Differentiation of hematopoietic stem cells to functional, multinucleated osteoclasts is driven by two essential cytokines, M-CSF, secreted by osteoblasts, and RANKL, found as a soluble factor or as a membrane-bound cytokine expressed on osteoblasts, osteocytes, dendritic cells, mature T-cells, and hematopoietic precursors.[19] In the simple system presented herein, it is possible that MMP-13 could process M-CSF and/or RANKL to more active forms, or MMP-13 could process RANK to improve binding of RANKL. However, other mechanisms are possible. Galectin-3, which suppresses osteoclastogenesis, is a substrate for MMP-13.[8] MMP-13 could process galectin-3 and inactivate it. MMP-13 activates proMMP-9, and the activation of proMMP-9 has been proposed to result in MMP-9 processing the core histone protein H3 *N*-terminal tail (H3NT) which then regulates gene pathways facilitating osteoclastogenesis.[20] While MMP-9 has been documented to be in the nucleus of primary osteoclast precursor-induced cells,[20] it is not clear where proMMP-9 is activated. Alternatively, MMP-9 activates TGFβ and promotes the cleavage of galectin-3, which would reduce the ability of galectin-3 to suppress osteoclastogenesis.[8, 21]

The *in vivo* mechanism by which MMP-13 facilitates osteoclastogenesis may be more complex. Recent studies indicated that osteoclast-mediated bone resorption required either MMP-9 or MT1-MMP, with each enzyme providing a functional redundancy for the other.[22] Co-culture of MDA-MB-231 breast cancer cells with MC3T3-E1 osteoblasts in a mineralized osteoid matrix resulted in an increase between 1.3- and 26-fold of 48 proteins or protein fragments in supernatants containing MMP-13.[23] MMP-13 inactivated chemokines CCL2 and CCL7, activated platelet-derived growth factor C (PDGF-C), and cleaved SAA3, osteoprotegerin, CutA, and antithrombin III.[23] CCL2, CCL7, PDGF-C, and SAA3 recruit osteoclasts and play a role in

osteoclast differentiation, but it is not clear how MMP-13 processing of these substrates impacts these activities.[23]

RF036 was previously shown to inhibit MMP-13 type II collagenolysis >90% at a compound concentration of 20 μM.[14b] We presently examined the dose-dependence of type II collagenolysis inhibition by RF036, and found near complete inhibition at a compound concentration of 250 nM (Figure 3). Inhibitors 1-4 were tested for their ability to inhibit MMP-13 type II collagenolysis over a range of concentrations from 1.52 nM to 10 μM. Inhibitor 1 inhibited collagenolysis only at high concentrations (3.33 and 10 μM) (Figure 4). Inhibitor 2 weakly inhibited collagenolysis at the highest concentration tested (10 μM) (Figure 4). Inhibitor 3 partially inhibited collagenolysis at the highest concentration tested (10 μM) (Figure 4). Inhibitor 4 (in either salt form) did not inhibit collagenolysis (Figure 4).

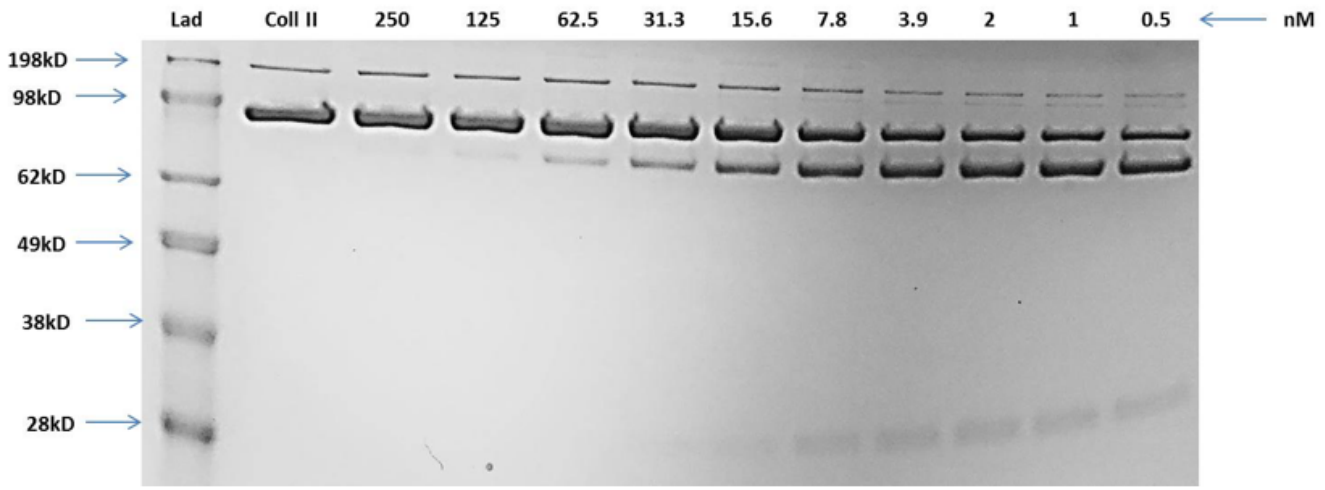

Figure 3. Inhibition of collagenolysis by RF036. The assay was initiated by dispensing 9 μL of 4 nM MMP-13 in EAB. Two μL of RF036 at varying concentrations in EAB were added and incubated with the enzyme for 30 min. Reactions were initiated by addition of 9 μL of 333 nM type II collagen in EAB. After 22 h of incubation at 37 °C, the samples were resolved by electrophoresis on an 8% SDS-PAGE gel.

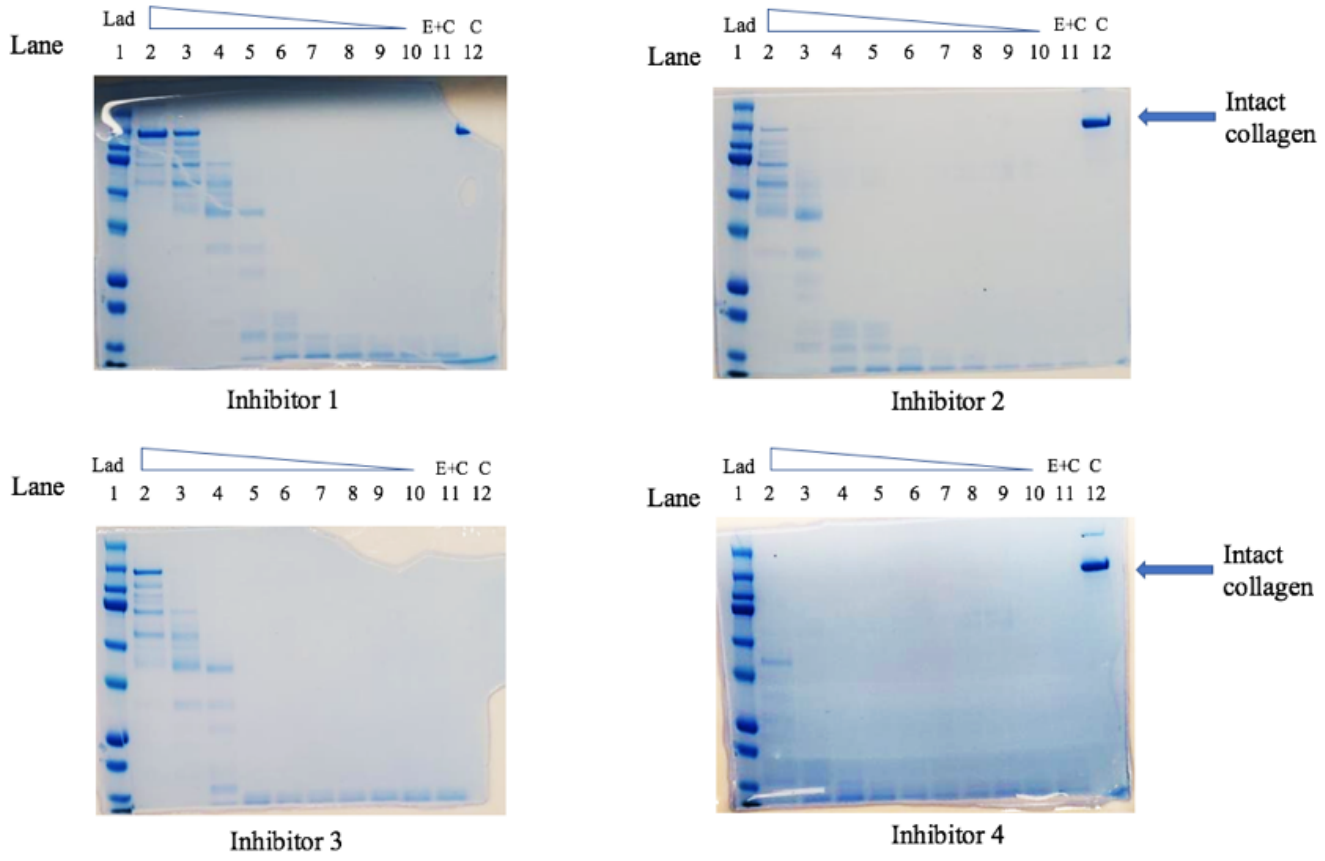

Figure 4. Inhibition of collagenolysis by inhibitors 1-4. The assay was initiated by dispensing 9 μL of 4 nM MMP-13 in EAB. Two μL of test compounds at varying concentrations in EAB were added and incubated with the enzyme for 30 min. Reactions were initiated by addition of 9 μL of 333 nM type II collagen in EAB. After 22 h of incubation at 37 °C, the samples were resolved by electrophoresis on an 8% SDS-PAGE gel. The inhibitor concentrations were 10 μM (lane 2), 3.3 μM (lane 3), 1.11 μM (lane 4), 370 nM (lane 5), 125 nM (lane 6), 41.2 nM (lane 7), 13.7 nM (lane 8), 4.57 nM (lane 9), and 1.52 nM (lane 10). MMP-13 plus type II collagen with no inhibitor (lane 11) and type II collagen with no MMP-13 or inhibitor (lane 12) are controls.

None of the four compounds were effective inhibitors of MMP-13 catalyzed type II collagenolysis (Figure 4). This result was particularly surprising, as RF036 inhibits type II collagenolysis effectively (Figure 3). Loss of inhibition of MMP-13 collagenolytic activity was not due to replacing the backbone sulfur atom with either carbon or nitrogen, as when the backbone sulfur in RF036 was replaced by either carbon or nitrogen inhibition of collagenolysis was retained.[14b] Thus, the oxetane and azetidine moieties impact the positioning of the inhibitor to render it ineffective towards collagenolysis. In our prior study,[14b] compound **33** was found to be a good inhibitor of MMP-13 activity towards a synthetic substrate (IC_{50} = 43.2 nM) but not towards collagenolysis (<10% at 20 μM inhibitor concentration). In similar fashion to the compounds described in the present study, compound **33** featured a bulky substitution for the methyl amine group of RF036. It is also possible that the combined substitutions within the present inhibitors are not independent, and thus the substitution of the backbone sulfur may impact inhibition of collagenolysis.

RF036 and inhibitors 1-4 are all based on the 2-(arylmethylthio)-cyclopentapyrimidin-4-one scaffold, which we initially described as a non-competitive MMP-13 inhibitor.[24] X-ray crystallographic structural analysis of this inhibitor family found binding to the MMP-13 S_1'* specificity pocket within the S_1' subsite.[14a, 24c] These leaves open the possibility that binding of a macromolecular substrate outside of the MMP-13 active site could dispel the inhibitor from or reorient the inhibitor within the S_1'* specificity pocket.

Summary and Conclusion

We synthesized four compounds based on the template of RF036, a highly selective MMP-13 inhibitor, in an attempt to obtain an inhibitor with an improved drug metabolism and pharmacokinetics (DMPK) profile. These new compounds have been evaluated for MMP-13 inhibition potency, protease selectivity, kinetic solubility, Caco-2 cell permeability, *in vitro* stability in human, rat, and mouse liver microsomes, and inhibition of osteoclastogenesis and collagenolysis. The overall goal was to reach the following *in vitro* values: (a) $K_i \leq 15$ nM while maintaining selectivity over other MMPs; (b) kinetic solubility higher than 15 μM; (c) ≥20 min *in vitro* half-life ($t_{1/2}$) in liver microsomes; and (d) permeability coefficients $\geq 2.0 \times 10^{-6}$ cm/sec.[25]

Inhibitor 3, in which the backbone sulfur and terminal methyl group of RF036 were replaced by nitrogen and oxetane, respectively, had comparable activity, selectivity, and membrane permeability to RF036 while exhibiting greatly enhanced solubility and stability. Inhibitor 3 effectively inhibited MMP-13-mediated osteoclastogenesis but spared collagenolysis.

The compounds presented herein may undergo further optimization. For example, the isopropyl group could be replaced by a cyclopropyl group. Based on our prior study, the cyclopropyl group could provide further enhancement of stability, no inhibition of CYP3A4, and greatly reduced inhibition of CYP2C9.[14b] One could also replace the amide bond to reduce compound degradation by proteases.

Multiple attempts to develop MMP inhibitor-based drugs failed mostly due to the dose limiting side effects collectively known as musculoskeletal syndrome (MSS).[26] While the exact cause of MSS is not known, it is believed to be due to the lack of selectivity of drug candidates towards other representatives of metalloproteinase families.[26b, 27] Importantly for the present work, selective MMP-13 inhibition does not induce MSS in rat models.[28]

Experimental Section

Synthesis of compounds

All materials were obtained from commercial suppliers and used without further purification unless otherwise noted. Anhydrous solvents were obtained from Sigma-Aldrich or Fisher Scientific and were used directly. All air or moisture sensitive reactions were carried out using oven-dried glassware under a nitrogen atmosphere. Reactions were monitored by either thin layer chromatography (TLC) or analytical LC-MS. TLC was performed on Kieselgel 60 F254 glass plates pre-coated with a 0.25 mm thickness of silica gel. TLC plates were visualized with UV light and/or by potassium permanganate and phosphomolybdic acid stains. Column chromatography was performed on a Combi flash automated system. Compound was loaded onto pre-filled cartridges filled with KP-Sil 50 μm irregular silica. NMR spectra were recorded on a 400 MHz spectrometer and measured in $CDCl_3$, MeOD-d_4, or DMSO-d_6 ($CHCl_3$: H, δ=7.26, C, δ=77.16, MeOH: H, δ=3.31, C, δ=49.00, DMSO: H, δ=2.50, C, δ=39.50). All ^{1}H and ^{13}C shifts are given in ppm and coupling constants *J* are given in Hz. Mass (m/z) of the compounds was determined using an UP-LC [Acquity H class] equipped with XBridge® BEH C18 XP 130 Å, 2.5 μm, 2.1 × 150 mm column and a LC-MS instrument (Agilent 1100 series LC with 500 Ion TrapMS) equipped with Zorbax RR SB-C18 80 Å, 3.5 μm, 4.6 × 100 mm column. Elution was performed using the following conditions: 5% (v/v) acetonitrile (+0.1% formic acid) in 95% (v/v) H_2O (+0.1% formic acid), ramped to 95% acetonitrile over 12 min, and holding at 95% acetonitrile for 3 min with a flow rate of 1 mL/min. The purity of each compound was ≥95% based on this analysis. Synthetic methods for the production of all inhibitors and inhibitor intermediates as well as characterization of all inhibitors is presented in the Supporting Information.

MMP-13 enzyme activation

Full-length recombinant human proMMP-13 was purchased from R&D Systems (catalog no. 511-MM; Minneapolis, MN). ProMMP-13 in 100 μL enzyme assay buffer (EAB; 50 mM Tris•HCl, pH 7.5, 100 mM NaCl, 10 mM $CaCl_2$, 0.05% Brij-35) was activated with 1 mM (p-aminophenyl)mercuric acid (APMA) for 2 h at 37 °C. The stock of active MMP-13 was diluted to 384.6 nM and stored at -80 °C.

Inhibitor kinetics

Our methods for kinetic evaluation of MMP inhibitors have been described in detail.[24b, 24c] Briefly, fTHP-15(FAM) [sequence (Gly-Pro-Hyp)$_5$-Gly-Pro-Lys(5-Fam)-Gly-Pro-Gln-Gly-Leu-Arg-Gly-Gln-Lys(Dabcyl)-Gly-Val-Arg-(Gly-Pro-Hyp)$_5$-NH_2, where Hyp = 4-hydroxy-L-proline, Fam = carboxyfluorescein, and Dabcyl = 4-(dimethylaminoazo)benzene-4-

carboxylic acid],[29] MMP-13, and inhibitor working solutions were prepared in EAB. All reactions were conducted in 384-well black polystyrene plates (Greiner, North Carolina, catalog no. 784076). Fluorescence was measured on a BioTek H1 microplate reader using $\lambda_{excitation}$ = 488 nm and $\lambda_{emission}$ = 520 nm. Rates of hydrolysis were obtained from plots of fluorescence versus time using data points from only the linear portion of the hydrolysis curve. To determine the IC_{50} value of each compound, the compounds were screened in 10-point 3-fold dilution dose-response curve format in triplicates. The assay began by dispensing 5 μL of test compounds in assay buffer followed by 5 μL of MMP-13. The enzyme was allowed to incubate with the test compounds for 30 min at 25 °C. The assays were initiated by addition of 5 μL of fTHP-15(FAM) and immediately placed in the microplate reader to record fluorescence. To determine IC_{50} values of each compound, the relative fluorescence units (RFU) from wells containing MMP-13, fTHP-15(FAM), and compounds were plotted versus no enzyme and untreated controls. For each compound, RFUs from the linear part of the curve were fitted with a four parameter equation describing a sigmoidal dose-response curve with adjustable baseline using GraphPad Prism® version 11 suite of programs. The IC_{50} values of the compounds were determined as the concentrations that resulted in 50% enzyme activity when compared to the activity of the control samples (without a compound). These values were generated from fitted curves by solving for the X-intercept at the 50% inhibition level of Y-intercept using the built-in dose-response model algorithm of GraphPad Prism (La Jolla, CA). Since the determination of IC_{50} values may vary from the true inhibitory values of a molecule, K_i were determined for the best compounds. Briefly, varying concentrations of inhibitor diluted in EAB were added to 384 well plates. MMP-13 (4 nM) and fTHP-15(FAM) were added. Since $K_{i(app)} = K_i (1 + [S]/K_M)$, the peptide was used at <5-10% K_M. This insured that $K_{i(app)}$ is a close approximation of K_i. Initial velocities (V_i) were expressed as relative fluorescence/time and monitored with increasing concentration of inhibitor. K_i values were calculated using GraphPad software. Data was collected at enzyme concentrations no greater than $10K_i$.

Selectivity assay

To determine the selectivity of each inhibitor, the compounds were tested against a protease panel consisting of MMP-1, MMP-2, MMP-8, MMP-9, and MMP-14/MT1-MMP. All enzymes were purchased from R&D Systems and activated according to manufacturer's instructions. Upon activation, each enzyme was diluted in EAB to 20 nM and stored at -80 °C until further use. The compounds were screened as described above in 10-point 3-fold dilution dose-response curve format in triplicate utilizing fTHP-15(FAM) as substrate except for MMP-1, for which Knight substrate [Mca-Lys-Pro-Leu-Gly-Leu-Lys(Dnp)-Ala-Arg-NH_2, where Mca is 7-methoxycoumarin-4-acetyl and Dnp is 2,4-dinitrophenyl] was used.[14]

Kinetic solubility

Compound solubility was determined by HPLC. Compounds were incubated at a concentration of 500 μM in PBS for 18 h with a vortex of 600 rpm. After the incubation period, samples were centrifuged for 10 min at 10000 rpm and supernatant analyzed by HPLC with peak area compared to standards of known concentration.

Metabolic stability in mouse, rat, and human liver microsomes[30]

Microsome stability was evaluated by incubating 1 μM compound or positive control (verapamil) with 1.0 mg/mL hepatic microsomal protein in 100 mM potassium phosphate buffer, pH 7.4. Solutions were held at 37 °C with continuous shaking. The reactions were initiated by adding NADPH to 1 mM final concentration. Reactions without NADPH at 0 and 60 min were also incubated to rule out non-NADPH metabolism or chemical instability in the incubation buffer. The final DMSO concentration was <0.1%. The final incubation volume was 300 μL and 40 μL aliquots were removed at 0, 5, 15, 30, and 60 min. Aliquots were added to 200 μL ice-cold acetonitrile (containing the internal standard 200 ng/mL telmisartan) to terminate the reaction and precipitate the protein. The vials were centrifuged at 4000 rpm for 20 min. The supernatants obtained were analysed on LC-MS/MS (Shimadzu-8040) to monitor the disappearance of compound. For the LC separation, the column was an XBridge 5 μm C_{18}, solvent A = 0.1% formic acid in 10 mM ammonium acetate, solvent B = methanol, and the flow rate = 0.6 mL/min. The data was log transformed and results reported as half-life ($t_{1/2}$).

Caco-2 permeability

Caco-2 human epithelial colorectal adenocarcinoma cells were plated in 24-Transwell® dual chamber plates (Millipore, Billerica, MA) (cell density of 60,000 cells/cm^2 on day-1). The permeability studies were conducted with the monolayers cultured for 21-22 days. The integrity of each Caco-2 cell monolayer was certified by trans epithelial electrical resistance (TEER) test (pre-experiment) and by determining the permeability of the reference compound, Lucifer yellow. Caco-2 cell monolayers with TEER values greater than 250 Ω/cm^2 were considered for experimentation. Propranolol and atenolol were used as positive controls for high and low permeable compounds, respectively. The concentration of compound used in the assay was 10 μM. The permeability assay buffer was Hanks Balanced Salt Solution (HBSS) containing 10 mM HEPES and 15 mM glucose at a pH of 7.4. The final concentration of DMSO in the spiking solution was 0.05%. The bidirectional permeability study was initiated by adding an appropriate volume of HBSS buffer containing compound to respective apical and basolateral chambers (n=2) [31]. An aliquot of sample (25 μL) was taken from both chambers at 0 and 60 min of the incubation period and to this 150 μL of acetonitrile with internal standard (200 ng/mL telmisartan) was added, mixed gently, and centrifuged at 4000 rpm (Eppendorf 5424R, Germany) for 20 min. An aliquot of 150 μL was subsequently transferred to the auto-sampler and injected for analysis on LC-MS/MS. Each determination was performed in duplicate. The flux of co-dosed Lucifer yellow was also measured for each monolayer to ensure no damage was inflicted to the cell monolayers during the flux period. The apparent permeability (P_{app}) and percent recovery were calculated as follows:

$$P_{app} = (dC_R/dt) \times V_R/(A \times C_A) \quad (1)$$

$$\text{Percent Recovery} = 100 \times ((V_R \times C_{Rfinal}) + (V_D \times C_{Dfinal}))/(V_D \times C_N) \quad (2)$$

where dC_R/dt was the slope of the cumulative concentration in the receiver compartment versus time in μM sec^{-1}; V_R was the volume of the receiver compartment in cm^3; V_D was the volume of the donor compartment in cm^3; A was the area of the insert; C_A was the average of the nominal dosing concentration and the measured 120 min donor concentration in μM; C_N was the nominal concentration of the dosing solution in μM; C_R final was the cumulative receiver concentration in μM at the end of the incubation period; and C_D final was the concentration of the donor in μM at the end of the incubation period.

***In vitro* osteoclast differentiation assays**

All animal experiments were performed in accordance with the guidelines of the Florida Atlantic University Institutional Animal Care and Use Committee (IACUC), protocol number A18-04. Osteoclastogenesis was performed as previously described.[32] Briefly, whole bone marrow was flushed from both tibia and femur in hind limbs of either male or female mice. The marrow was plated at 0.5 x 10^6 cells/mL in αMEM supplemented with 25 ng/mL recombinant macrophage-colony stimulating factor (rM-CSF) (R&D Systems, Minneapolis, MN). After 72 h, non-adherent cell population was plated at 1 x 10^5 cells/250 μL/well in a 48 well plate in fresh media containing 25 ng/mL rM-CSF and 100 ng/mL RANKL. Inhibitors were added in triplicates at 10 μM final concentration at the time of plating. Media was refreshed every 2-3 d for 5-7 d. Upon osteoclast formation, cells were fixed by incubating in 4% paraformaldehyde for 10 min at room temperature. Samples were subsequently stained with TRAcP stain (Sigma-Aldrich, St. Louis, MO) per manufacturer instructions.

Multinucleated osteoclasts were counted over 5 images from each triplicate sample.

Type II collagen assay

To assess the potency of probes using a physiologically relevant substrate we tested compounds in an assay utilizing type II collagen (Sigma-Aldrich, St. Louis, MO, Cat# 234184). All experiments were performed in 384-well white microtiter plates. The assay was initiated by dispensing 9 μL of 4 nM MMP-13 in EAB. Two μL of test compounds in EAB were added and incubated with the enzyme for 30 min. Reactions were initiated by addition of 9 μL of 333 nM type II collagen in EAB. After 22 h of incubation at 37 °C, the samples were resolved by electrophoresis on an 8% SDS-PAGE gel. The gel was stained with Coomassie Blue and band intensities quantified versus no-enzyme and untreated controls.

Acknowledgements

This research was supported by NIH R01 grant CA239214 (GBF) and an FAU Undergraduate Research Grant (GD). We acknowledge Acubiosys Private Limited, Hyderabad, India, for performing the kinetic solubility, metabolic stability, and Caco-2 permeability assays.

Keywords: matrix metalloproteinase • matrix metalloproteinase inhibitor • breast cancer • bone metastasis • osteoclastogenesis

[1] E. Gobin, K. Bagwell, J. Wagner, D. Mysona, S. Sandirasegarane, N. Smith, S. Bai, A. Sharma, R. Schleifer, J. X. She, *BMC Cancer* **2019**, *19*, 581.

[2] J. M. P. Freije, T. Diez-Itza, M. Balbin, L. M. Sanchez, R. Blasco, J. Tolivia, C. Lopez-Otin, *J. Biol. Chem.* **1994**, *269*, 16766-16773.

[3] H.-J. Chang, M.-J. Yang, Y.-H. Yang, M.-F. Hou, E.-J. Hsueh, S.-R. Lin, *Oncol. Rep.* **2009**, *22*, 1119-1127.

[4] B. Zhang, X. Cao, Y. Liu, W. Cao, F. Zhang, S. Zhang, H. Li, L. Ning, L. Fu, Y. Niu, R. Niu, B. Sun, X. Hao, *BMC Cancer* **2008**, *8*, 83.

[5] a) S. Paget, *Cancer Metastasis Rev.* **1989**, *8*, 98-101; b) M. Tauro, C. C. Lynch, *Cancers* **2018**, *10*, 185.

[6] G. R. Mundy, *Nat. Rev. Cancer* **2002**, *2*, 584-593.

[7] T. Ohshiba, C. Miyaura, M. Inada, A. Ito, *Br. J. Cancer* **2003**, *88*, 1318-1326.

[8] E. Pivetta, M. Scapolan, M. Pecolo, B. Wassermann, I. Abu-Rumeileh, L. Balestreri, E. Borsatti, C. Tripodo, A. Colombatti, P. Spessotto, *Breast Cancer Res.* **2011**, *13*, R105.

[9] J. A. Blagg, M. C. Noe, L. A. Wolf-Gouveia, L. A. Reiter, E. R. Laird, S. P. Chang, D. E. Danley, J. T. Downs, N. C. Elliott, J. D. Eskra, R. J. Griffiths, J. R. Hardink, A. I. Hauget, C. S. Jones, J. L. Liras, L. L. Lopresti-Morrow, P. G. Mitchell, J. Pandit, R. P. Robinson, C. Subramanyam, M. L. Vaughn-Bowser, S. A. Yocum, *Bioorg. Med. Chem. Lett.* **2005**, *15*, 1807-1810.

[10] M. Shah, D. Huang, T. Blick, A. Connor, L. A. Reiter, J. R. Hardink, C. C. Lynch, M. Waltham, E. W. Thompson, *PLoS One* **2012**, *7*, e29615.

[11] A. Lin, C. J. Giuliano, A. Palladino, K. M. John, C. Abramowicz, M. L. Yuan, E. L. Sausville, D. A. Lukow, L. Liu, A. R. Chait, Z. C. Galluzzo, C. Tucker, J. M. Sheltzer, *Sci. Transl. Med.* **2019**, *11*, eaaw8412.

[12] a) A. Saghatelian, N. Jessani, A. Joseph, M. Humphrey, B. F. Cravatt, *Proc. Natl. Acad. Sci. USA* **2004**, *101*, 10000-10005; b) P. Cuniasse, L. Devel, A. Makaritis, F. Beau, D. Georgiadis, M. Matziari, A. Yiotakis, V. Dive, *Biochimie* **2005**, *87*, 393-402.

[13] a) J. M. Chen, F. C. Nelson, J. I. Levin, D. Mobilio, F. J. Moy, R. Nilakantan, A. Zask, R. Powers, *J. Am. Chem. Soc.* **2000**, *122*, 9648-9654; b) C. K. Engel, B. Pirard, S. Schimanski, R. Kirsch, J. Habermann, O. Klingler, V. Schlotte, K. U. Weithmann, K. U. Wendt, *Chem. Biol.* **2005**, *12*, 181-189; c) L. A. Reiter, K. D. Freeman-Cook, C. S. Jones, G. J. Martinelli, A. S. Antipas, M. A. Berliner, K. Datta, J. T. Downs, J. D. Eskra, M. D. Forman, E. M. Greer, R. Guzman, J. R. Hardink, F. Janat, N. F. Keene, E. R. Laird, J. L. Liras, L. L. Lopresti-Morrow, P. G. Mitchell, J. Pandit, D. Robertson, D. Sperger, M. L. Vaughn-Bower, D. M. Waller, S. A. Yocum, *Bioorg. Med. Chem. Lett.* **2006**, *16*, 5822-5826; d) A. R. Johnson, A. G. Pavlovsky, D. F. Ortwine, F. Prior, C.-F. Man, D. A. Bornemeier, C. A. Banotai, W. T. Mueller, P. McConnell, C. Yan, V. Baragi, C. Lesch, W. H. Roark, M. Wilson, K. Datta, R. Guzman, H.-K. Han, R. D. Dyer, *J. Biol. Chem.* **2007**, *282*, 27781-27791; e) J. J. Li, J. Nahra, A. R. Johnson, A. Bunker, P. O'Brien, W.-S. Yue, D. F. Ortwine, C.-F. Man, V. Baragi, K. Kilgore, R. D. Dyer, H.-K. Han, *J. Med. Chem.* **2008**, *51*, 835-841; f) A. Heim-Riether, S. J. Taylor, S. Liang, D. A. Gao, Z. Xiong, E. M. August, B. K. Collins, B. T. Farmer, II, K. Haverty, M. Hill-Drzewi, H.-D. Junker, S. M. Margarit, N. Moss, T. Neumann, J. R. Proudfoot, L. Smith Keenan, R. Sekul, Q. Zhang, J. Li, N. A. Farrow, *Bioorg. Med. Chem. Lett.* **2009**, *19*, 5321-5324; g) D. A. Gao, Z. Xiong, A. Heim-Riether, L. Amodeo, E. M. August, X. Cao, L. Ciccarelli, B. K. Collins, K. Harrington, K. Haverty, M. Hill-Drzewi, X. Li, S. Liang, S. M. Margarit, N. Moss, N. Nagaraja, J. Proudfoot, R. Roman, S. Schlyer, L. S. Keenan, S. Taylor, B. Wellenzohn, D. Wiedenmayer, J. Li, N. A. Farrow, *Bioorg. Med. Chem. Lett.* **2010**, *20*, 5039-5043; h) D. Piecha, J. Weik, H. Kheil, G. Becher, A. Timmermann, A. Jaworski, M. Burger, M. W. Hofmann, *Inflamm. Res.* **2010**, *59*, 379-389; i) A. Jüngel, C. Ospelt, M. Lesch, M. Thiel, T. Sunyer, O. Schorr, B. A. Michel, R. E. Gay, C. Kolling, C. Flory, S. Gay, M. Neidhart, *Ann. Rheum. Dis.* **2010**, *69*, 898-902; j) C. Gege, B. Bao, H. Bluhm, J. Boer, B. M. Gallagher, B. Korniski, T. S. Powers, C. Steeneck, A. G. Taveras, V. M. Baragi, *J. Med. Chem.* **2012**, *55*, 709-716; k) T. Fischer, R. Riedl, *ChemMedChem* **2013**, *8*, 1457-1461; l) H. Nara, K. Sato, T. Naito, H. Mototani, H. Oki, Y. Yamamoto, H. Kuno, T. Santou, N. Kanzaki, J. Terauchi, O. Uchikawa, M. Kori, *Bioorg. Med. Chem.* **2014**, *22*, 5487-5505; m) H. Nara, K. Sato, T. Naito, H. Mototani, H. Oki, Y. Yamamoto, H. Kuno, T. Santou, N. Kanzaki, J. Terauchi, O. Uchikawa, M. Kori, *J. Med. Chem.* **2014**, *57*, 8886-8902; n) J. Lanz, R. Riedl, *ChemMedChem* **2015**, *10*, 451-454; o) H. Nara, K. Sato, A. Kaieda, H. Oki, H. Kuno, T. Santou, N. Kanzaki, J. Terauchi, O. Uchikawa, M. Kori, *Bioorg. Med. Chem.* **2016**, *24*, 6149-6165; p) P. G. Ruminski, M. Massa, J. Strohbach, C. E. Hanau, M. Schmidt, J. A. Scholten, T. R. Fletcher, B. C. Hamper, J. N. Carroll, H. S. Shieh, N. Caspers, B. Collins, M. Grapperhaus, K. E. Palmquist, J. Collins, J. E. Baldus, J. Hitchcock, H. P. Kleine, M. D. Rogers, J. McDonald, G. E. Munie, D. M. Messing, S. Portolan, L. O. Whiteley, T. Sunyer, M. E. Schnute, *J. Med. Chem.* **2016**, *59*, 313-327; q) X.-W. Xie, R.-Z. Wan, Z.-P. Liu, *ChemMedChem* **2017**, *12*, 1157-1168; rT. Fischer, R. Riedl, *ChemistryOpen* **2017**, *6*, 192-195.

[14] a) J. Y. Choi, R. Fuerst, A. M. Knapinska, A. Taylor, L. Smith, X. Cao, P. J. Hart, G. B. Fields, W. R. Roush, *J. Med. Chem.* **2017**, *60*, 5816-5825; b) R. Fuerst, J. Y. Choi, A. M. Knapinska, L. Smith, M. D. Cameron, C. H. Ruiz, G. B. Fields, W. R. Roush, *Bioorg. Med. Chem.* **2018**, *26*, 4984-4995.

[15] a) C. A. Lipinski, F. Lombardo, B. W. Dominy, P. J. Feeney, *Adv. Drug Deliver. Rev.* **1997**, *23*, 3-25; b) H. van de Waterbeemd, E. Gifford, *Nat. Rev. Drug Discov.* **2003**, *2*, 192-204.

[16] H. van de Waterbeemd, D. A. Smith, K. Beaumont, D. K. Walker, *J. Med. Chem.* **2001**, *44*, 1313-1333.

[17] L. Fredlund, S. Winiwarter, C. Hilgendorf, *Mol. Pharm.* **2017**, *14*, 1601-1609.

[18] S. G. Almalki, D. K. Agrawal, *Stem Cell Res. Ther.* **2016**, *7*, 129.

[19] a) T. A. Guise, J. M. Chirgwin, *Clin. Orthop. Relat. Res.* **2003**, *415 Suppl.*, S32-S38; b) S. Marino, J. G. Logan, D. Mellis, M. Capulli, *Bonekey Rep.* **2014**, *3*, 570.

[20] K. Kim, V. Punj, J.-M. Kim, S. Lee, T. S. Ulmer, W. Lu, J. C. Rice, W. An, *Genes Develop.* **2016**, *30*, 208-219.

[21] K. C. Nannuru, M. Futakuchi, M. L. Varney, T. M. Vincent, E. G. Marcusson, R. K. Singh, *Cancer Res.* **2010**, *70*, 3494-3504.

[22] L. Zhu, Y. Tang, X. Y. Li, E. T. Keller, J. Yang, J. S. Cho, T. Y. Feinberg, S. J. Weiss, *Sci. Transl. Med.* **2020**, *12*, eaaw6143.

[23] C. Morrison, S. Mancini, J. Cipollone, R. Kappelhoff, C. Roskelley, C. Overall, *J. Biol. Chem.* **2011**, *286*, 34271-34285.

[24] a) J. L. Lauer-Fields, D. Minond, P. S. Chase, P. E. Baillargeon, S. A. Saldanha, R. Stawikowska, P. Hodder, G. B. Fields, *Bioorg. Med. Chem.* **2009**, *17*, 990-1005; b) J. Roth, D. Minond, E. Darout, Q. Liu, J. Lauer, P. Hodder, G. B. Fields, W. R. Roush, *Bioorg. Med. Chem. Lett.* **2011**, *21*, 7180-7184; c) T. P. Spicer, J. Jiang, A. B. Taylor, P. J. Hart, W. R. Roush, G. B. Fields, P. S. Hodder, D. Minond, *J. Med. Chem.* **2014**, *57*, 9598-9611.

[25] a) L. Di, E. H. Kerns, *Curr. Opin. Drug Discov. Devel.* **2005**, *8*, 495-504; b) F. Madoux, X. Li, P. Chase, G. Zastrow, M. D. Cameron, J. J. Conkright, G. R. Griffin, S. Thacher, P. Hodder, *Mol. Pharmacol.* **2008**, *73*, 1776-1784; c) X. Li, X. Song, T. M. Kamenecka, M. D. Cameron, *Drug Metab. Dispos.* **2012**, *40*, 1803-1809.

[26] a) P. S. Burrage, K. S. Mix, C. E. Brinckerhoff, *Front. Biosci.* **2006**, *11*, 529-543; b) B. Fingleton, *Semin. Cell Dev. Biol.* **2008**, *19*, 61-68; c) H. Takaishi, T. Kimura, S. Dalal, Y. Okada, J. D'Armiento, *Curr. Pharm. Biotechnol.* **2008**, *9*, 47-54; d) M. Tauro, J. McGuire, C. C. Lynch, *Cancer Metastasis Rev.* **2014**, *33*, 1043-1057.

[27] a) J. T. Peterson, *Cardiovasc. Res.* **2006**, *69*, 677-687; b) C. M. Overall, O. Kleifeld, *Br. J. Cancer* **2006**, *94*, 941-946; c) C. M. Overall, O. Kleifeld, *Nat. Rev. Cancer* **2006**, *6*, 227-239.

[28] V. M. Baragi, G. Becher, A. M. Bendele, R. Biesinger, H. Bluhm, J. Boer, H. Deng, R. Dodd, M. Essers, T. Feuerstein, B. M. Gallagher, Jr., C. Gege, M. Hochgürtel, M. Hofmann, A. Jaworski, L. Jin, A. Kiely, B. Korniski, H. Kroth, D. Nix, B. Nolte, D. Piecha, T. Powers, F. Richter, M. Schneider, C. Steeneck, I. Sucholeiki, A. Taveras, A. Timmermann, J. Van Veldhuizen, J. Weik, X. Wu, B. Xia, *Arthritis Rheum.* **2009**, *60*, 2008-2018.

[29] M. Tokmina-Roszyk, D. Tokmina-Roszyk, G. B. Fields, *Biopolymers (Pept. Sci.)* **2013**, *100*, 347-355.

[30] R. S. Obach, *Drug Metabolism Disposition* **1999**, *27*, 1350-1359.

[31] P. V. Balimane, Y. H. Han, S. Chong, *J. AAPS* **2006**, *8*, E1-E13.

[32] G. Shay, M. Tauro, F. Loiodice, P. Tortorella, D. M. Sullivan, L. A. Hazlehurst, C. C. Lynch, *Oncotarget* **2017**, *8*, 41827-41840.

Entry for the Table of Contents

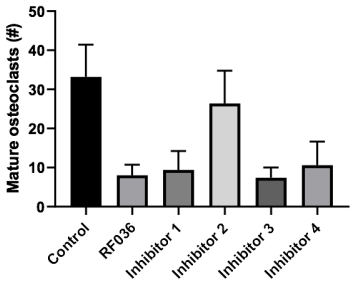

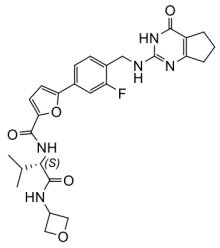

The development of matrix metalloproteinase 13 (MMP-13) inhibitors has often been marred by poor PK properties of resulting compounds. The present study has sought to improve the PK properties of RF036, a previously described selective MMP-13 inhibitor. Inhibitor 3 had more favorable PK properties than RF036 and was an effective inhibitor of osteoclastogenesis, a critical process that occurs during breast cancer metastasis to the bone.